Regulating Voltage Magnitude and Phase Imbalance using DERs via Volt/VAR Control Rules

Ashutossh Gupta
Elmore Family School of ECE
Purdue University
West Lafayette, IN
gupta799@purdue.edu

Jinlei Wei
Elmore Family School of ECE
Purdue University
West Lafayette, IN
wei474@purdue.edu

Vassilis Kekatos
Elmore Family School of ECE
Purdue University
West Lafayette, IN
kekatos@purdue.edu

***Abstract*—Fluctuations of active power injections by rooftop photovoltaics (PVs) and distributed energy resources (DERs) challenge voltage regulation in distribution grids. Reactive power support by DERs following Volt/VAR (VVR) rules driven by local data has been advocated as an effective fast-response mechanism to regulate voltage. Customizing the parameters of VVR rules is a non-trivial task for grid operators as VVR rules give rise to nonlinear dynamics and should operate under diverse and uncertain loading conditions. Existing works typically resort to linearized models of presumably balanced grids, and design VVR rules to regulate voltage magnitudes alone. Under the practical setting of single-phase DERs operating over unbalanced feeders modeled according to the exact AC power flow equations, injecting reactive power to regulate voltage could aggravate voltage phase imbalance issues. This work optimally designs VVR rules to regulate voltage and reduce voltage unbalance factors (VUF) in multiphase distribution grids. To avoid mixed-integer programs, we formulate a stochastic optimization program and surrogate chance constraints by smooth approximations. The program is solved via an iterative primal-dual algorithm, for which gradients are computed via implicit differentiation at grid equilibrium states. Numerical tests corroborate that if properly designed, VVR rules can regulate voltage magnitudes and phase imbalance alike.**

***Index Terms*—IEEE Standard 1547, Volt/VAR control rules, chance constraints, multiphase feeders, ohmic line losses.**

I. Introduction

[1] With the proliferation of PVs and DERs following frequency regulation signals, voltage regulation is exacerbated in modern power distribution grids. Although reactive power control has been deemed an effective means of regulating voltage, deciding the reactive power setpoints for thousands of DERs in near real-time can be technically challenging. Reactive power setpoints could be optimally determined by solving an optimal power flow (OPF) at the control center [1]. Nonetheless, this strategy entails computational burden and communication delays. As a subpar yet fast-responding mechanism, the IEEE Std. 1547 suggests that reactive power setpoints should be decided autonomously by each DER based on local data and predetermined control rules [2], [3]. Among the options of constant VAR, fixed power factor, Watt/VAR [4], and Volt/VAR (VVR) control, the latter may be the most effective given that voltage depends on grid-wide conditions and is the quantity under control, anyway. This work deals with the task of *optimal rule design* (ORD) of VVR control on multiphase distribution feeders.

Although the standard specifies that VVR rules should be particular non-increasing and piecewise-linear functions of local voltage magnitudes, their precise form is left for the grid operator to determine. The operator could customize VVR rules per node and update them periodically based on the anticipated grid loading scenarios [5]. The task of ORD is technically challenging as it involves nonlinear dynamics and uncertain grid conditions. Under VVR dynamics, stability is non-trivial to ensure, and the grid equilibrium state is hard to incorporate into optimization formulations [6], [7]. One approach is to capture the piecewise-linear rules using binary decision variables and formulate ORD as a mixed-integer program [8]–[10]. Unfortunately, these models scale unfavorably with the problem size and involve products between continuous variables for which McCormick relaxation is known not to be exact. Alternatively, ORD can be handled using gradient-based continuous optimization to pursue local minima. These approaches involve computing gradients of grid quantities (such as ohmic losses or voltage magnitudes) with respect to the VVR rule parameters, all evaluated at the grid equilibrium point under VVR dynamics. Under linearized grid models, such gradients have been computed efficiently leveraging automatic differentiation upon reformulating VVR dynamics as recursive neural networks (RNNs) [5], [11].

Most existing ORD studies resort to linearized grid models, are confined to single-phase or balanced multiphase distribution feeders, and/or target only regulating voltage magnitudes within specified limits [12]–[15]. Industry practice, however, entails single-phase DERs operating on multiphase untransposed feeders. Although operators may allocate DERs uniformly across phases while approving interconnection, real-time conditions could give rise to unbalanced conditions. Departures of three-phase voltages from a balanced set could compromise the operation of large three-phase motors. Severely unbalanced power injections at feeder heads could complicate transmission-level operations. Reference [16] puts forth a VAR control scheme at the inverter level to minimize phase imbalance, and [17] formulates a chance-constrained AC-OPF problem to decide optimal DER setpoints, yet not VVR rules. Designing VVR rules to regulate voltage magnitude could exacerbate voltage phase imbalance. Therefore,

[1]Work supported in part by US NSF grants 2500682.

voltage magnitude regulation and voltage phase imbalance should be carefully considered during ORD.

Having identified the gaps mentioned above, this work advances ORD in three aspects: *c1)* It designs stable VVR rules that jointly mitigate voltage phase imbalance and regulate voltage magnitudes while minimizing ohmic losses; *c2)* The ORD design relies on the exact AC power flow (PF) model of multiphase distribution feeders; and *c3)* To improve on computational complexity, gradients are computed using implicit rather than automatic differentiation. Numerical tests corroborate that the proposed ORD algorithms find VVR rules that can successfully regulate voltage magnitude and imbalance simultaneously.

The rest of the paper is organized as follows. Section II formulates a stochastic ORD problem. Section III derives mathematically amenable formulations for voltage magnitude and phase imbalance chance constraints. Section IV presents the proposed primal-dual algorithm. Numerical tests are provided in Section V and the work is concluded in Section VI.

II. Problem Formulation

Consider a multiphase radial distribution feeder with $B+1$ buses collected in set $\mathcal{B}$. The substation bus is indexed by 0. A bus can be multi-phase or single-phase. Each phase in a bus is called a *node* and is indexed by $n \in \mathcal{N} := \{1, \ldots, N\}$. The set $\mathcal{N}$ excludes the three nodes corresponding to the phases of the substation bus. DERs may be present at some or all nodes. Let vectors $\mathbf{u}$ and $\mathbf{v}$ collect the complex voltage phasors u_n and voltage magnitudes v_n for every node $n \in \mathcal{N}$. Let the set $\mathcal{M} \subset \mathcal{B}$ contain the index of buses that host multiple phases, and vector $\mathbf{u}_m = [u_m^a u_m^b u_m^c]$ carry the voltage phasors in all three phases of bus m for any $m \in \mathcal{M}$.

Let vector $\mathbf{s}_g = \mathbf{p}_g + j\mathbf{q}_g$ collect the complex power generated by DERs at all node. Vector $\mathbf{p}_g$ denotes the fixed real power generated by DERs (generally at the maximum power point), and $\mathbf{q}_g$ denotes the controllable reactive power to be designed. The power consumed by fixed loads at each node is stacked in vector $\mathbf{s}_l = \mathbf{p}_l + j\mathbf{q}_l$. The vector of complex power injections across the feeder can be decomposed as

$$\mathbf{s} = \mathbf{s}_g - \mathbf{s}_l = (\mathbf{p}_g - \mathbf{p}_l) + j(\mathbf{q}_g - \mathbf{q}_l) = \mathbf{p} + j\mathbf{q}.$$

The mapping from complex power injections to complex voltages is the inverse mapping of the AC power flow equations. In other words, given the substation voltage and the complex power injections $\mathbf{s}$, vector $\mathbf{u}$ can be found upon solving the power flow problem if the latter is feasible. This inverse power mapping will be abstractly denoted as

$$\mathbf{u} = \mathbf{F}(\mathbf{q}_g; \boldsymbol{\theta}) \tag{1}$$

where $\mathbf{q}_g$ are the reactive power injections to be controlled, and vector $\boldsymbol{\theta}$ collects the uncontrolled power injections $(\mathbf{p}_g, \mathbf{p}_l, \mathbf{q}_l)$. Each $\boldsymbol{\theta}$ corresponds to a *grid loading scenario*. We will slightly abuse notation and henceforth refer to $\mathbf{q}_g$ simply as $\mathbf{q}$, given that $\mathbf{q}_l$ is included in $\boldsymbol{\theta}$ anyway.

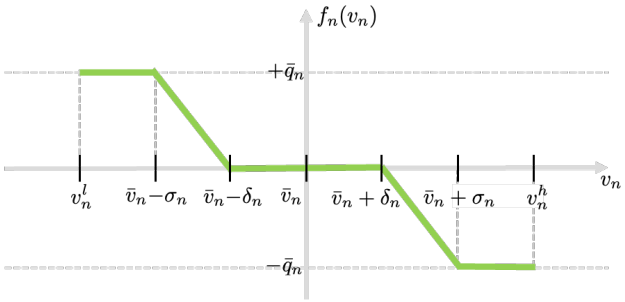

Fig. 1. A VVR control rule suggested by IEEE Std. 1547 [2].

The goal is to control reactive power injections $\mathbf{q}$ by DERs to regulate voltage. One way to control reactive power injections by DERs autonomously is through *Volt/VAR (VVR)* rules. As specified by the IEEE Std. 1547 [2], the reactive power injected by each DER can be determined by a piecewise-linear, non-increasing function of its local voltage magnitude $q_n = f_n(v_n)$ like the one illustrated in Fig. 1. To simplify ORD, let us assume that the rule f_n is odd symmetric around the nominal voltage $\bar{v}_n$ so that it can be described by four parameters $(\bar{v}_n, \delta_n, \sigma_n, \bar{q}_n)$. The last three parameters are used to describe the negative slope of the decreasing segment $\alpha_n = \frac{\bar{q}_n}{\sigma_n - \delta_n} > 0$. The standard determines the general shape of the rules by constraining parameters [2]:

$$0.95 \leq \bar{v}_n \leq 1.05 \tag{2a}$$
$$0 \leq \delta_n \leq 0.03 \tag{2b}$$
$$\delta_n + 0.02 \leq \sigma_n \leq 0.18 \tag{2c}$$
$$0 \leq \bar{q}_n \leq \hat{q}. \tag{2d}$$

for all DERs. Nevertheless, the grid operator can customize the exact shape of VVR rules. Let vector $\mathbf{z}$ collect the VVR parameters for all nodes hosting DERs.

Determining voltages $\mathbf{u}$ and DER reactive power injections $\mathbf{q}$ entails solving the AC-PF problem for multiphase systems $\mathbf{F}$ [18], iteratively along with the Volt/VAR dynamics f until convergence. This gives rise to the discrete-time non-linear dynamical system

$$\mathbf{u}^t = \mathbf{F}(\mathbf{q}^t; \boldsymbol{\theta}) \tag{3a}$$
$$q_n^{t+1} = f_n(v_n^t), \ \forall n \in \mathcal{N} \tag{3b}$$

According to [7], [19], and under a linearized grid model, the dynamical system of (3) enjoys exponential stability provided $\| \operatorname{dg}(\boldsymbol{\alpha})\mathbf{J}\|_2 < 1$, where matrix $\mathbf{J}$ contains the rows and columns of the Jacobian matrix $\nabla_{\mathbf{q}}\mathbf{u}$ corresponding to the nodes that host DERs, and $\operatorname{dg}(\boldsymbol{\alpha})$ is a diagonal matrix that carries the slope parameters across all DER nodes on its main diagonal. Because optimization solvers cannot handle strict inequalities, the VVR stability condition can be tightened as $\| \operatorname{dg}(\boldsymbol{\alpha})\mathbf{J}\|_2 \leq 1 - \epsilon$ for a small positive ϵ. The spectral norm in the stability condition gives rise to a linear matrix inequality constraint. To avoid this complication, the stability constraint can be inner approximated by a set of linear inequalities [5]:

$$|\mathbf{J}|^T \boldsymbol{\alpha} \leq (1 - \epsilon)\mathbf{1} \tag{4a}$$

$$0 \leq \alpha_n \leq \frac{1-\epsilon}{\sum_{m\in\mathcal{N}} J_{nm}},\ \forall n \in \mathcal{N}. \tag{4b}$$

Therefore, in addition to the constraints imposed by the IEEE standard in (2), VVR rule parameters should also satisfy the stability constraints in (4). In other words, the feasible set of VVR parameters $\mathbf{z}$ is defined as:

$$\mathcal{Z}_\epsilon := \{\mathbf{z} \text{ satisfying (2) and (4)}\}.$$

At equilibrium, voltages $\mathbf{u}^*$ and power injections $\mathbf{q}^*$ satisfy

$$\mathbf{u}^* = \mathbf{F}(\mathbf{q}^*; \boldsymbol{\theta}) \tag{5a}$$

$$q_n^* = f_n(v_n^*),\ \forall n \in \mathcal{N}. \tag{5b}$$

To compute voltages and power injections at equilibrium under scenario $\boldsymbol{\theta}$, one has to iterate between solving the power flow (PF) problem in (5a) and applying the VVR rules in (5b). The equilibrium voltage magnitude at node n is not necessarily $\bar{v}_n$. Hence, the PF equations cannot capture the equilibrium grid state, and VVR rules cannot be designed by standard optimal power flow (OPF) formulations.

We aim to optimize VVR rules per grid node for the following few hours. The grid operator designs the rules centrally once every few hours. Because the VVR control rules should perform reasonably well despite the uncertainty of load and solar injections, the grid operator may design these curves based on a dataset of grid loading scenarios deemed representative for the ensuing 2-4 hours. This task can be posed as a stochastic optimization problem

$$\min_{\mathbf{z}\in\mathcal{Z}_\epsilon} \quad \mathbb{E}_{\boldsymbol{\theta}}[\ell(\mathbf{u}^*(\mathbf{z};\boldsymbol{\theta}))] \tag{6a}$$

$$\text{subject to (s.to)} \quad \Pr_{\boldsymbol{\theta}}(g_c(\mathbf{u}^*(\mathbf{z};\boldsymbol{\theta}))) \geq 1-\beta,\ \forall c \in \mathcal{C} \tag{6b}$$

where the expectation operator is taken over the distribution of $\boldsymbol{\theta}$ and subscript c indexes constraints enforced per bus or node. All constraint indices c are collected in set $\mathcal{C}$. Function $l(\mathbf{u}^*(\mathbf{z};\boldsymbol{\theta}))$ appearing in the objective denotes the ohmic power losses on distribution lines. Function $g_c(\mathbf{u}^*(\mathbf{z};\boldsymbol{\theta}))$ can be interpreted as bounding the voltage magnitude at nodes within limits or maintaining the voltage imbalance between phases. Constraint (6b) ensures voltages have allowable values with a probability of at least $1-\beta$. Here, $\beta \in (0,1)$ is a small constant modeling the allowable constraint violation probability. The objective functions are evaluated at the equilibrium of the nonlinear dynamical system in (3).

A similar problem was addressed in [5], [11]. However, those earlier studies were restricted to single-phase feeders, presumed a linearized grid model, and leveraged automatic differentiation (AD) to compute gradients. Unfortunately, AD can become inefficient under an exact AC grid model as solving every PF appearing in (5b) involves another internal loop of PF solver iterations. This work considers the more practical setting of multiphase feeders and incorporates voltage phase imbalance metrics under the exact AC grid model. Further, it replaces automatic with implicit differentiation; i.e., gradients are computed via total differentiation at the equilibrium. We next explain how chance constraints are surrogated by differentiable functions to eventually approximately solve (6) using a primal-dual algorithm.

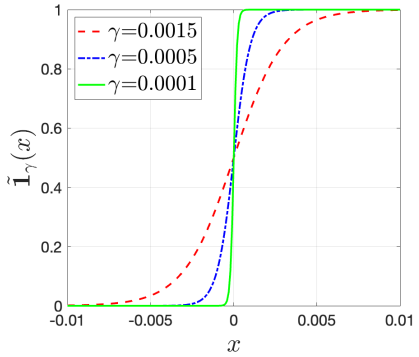

Fig. 2. Logistic function approximation of the unit step function.

III. Smooth Approximation of Chance Constraints

Suppose one of the constraints in (6b) ensures that the probability of voltage magnitude v_n lying within the desirable range of $[0.97, 1.03]$ pu is larger than $1-\beta_1$:

$$\Pr_{\boldsymbol{\theta}}(|v_n(\mathbf{z};\boldsymbol{\theta}) - 1| \leq 0.03) \geq 1-\beta_1,\ \forall n \in \mathcal{N} \tag{7}$$

for a small $\beta_1 > 0$. Although the constraint is evaluated at the equilibrium grid state, superscript * has been dropped for simplicity. The voltage magnitude deviations can be squared to obtain the equivalent constraint

$$\Pr((v_n(\mathbf{z};\boldsymbol{\theta}) - 1)^2 - 0.03^2 \leq 0) \geq 1-\beta_1,\ \forall n \in \mathcal{N}. \tag{8}$$

We would like to approximate this chance constraint by one captured by a differentiable function. To this end, first note that for a random variable x, it holds that

$$\Pr(x \geq 0) = \mathbb{E}\left[u(x)\right]$$

where $u(x)$ is the unit step function. Because $u(x)$ is nonsmooth, it is often replaced by the logistic function

$$\tilde{\mathbb{1}}_\gamma(x) := \frac{1}{1+e^{-x/\gamma}} \tag{9}$$

where parameter $\gamma > 0$ controls the closeness of the logistic function to the step function (see Figure 2). Using the logistic function and upon some algebraic manipulations, constraint (8) can be approximated by [11]:

$$\mathbb{E}\left[\tilde{\mathbb{1}}_\gamma\left((v_n-1)^2 - 0.03^2\right)\right] \leq \beta_1. \tag{10}$$

Even though most prior works on DER reactive power control focus on regulating voltage magnitudes, voltage imbalance can also be an essential issue. Among different metrics [17], voltage imbalance can be quantified by the so-termed *voltage unbalance factor* (VUF) on a three-phase bus, defined as the ratio of negative- to positive-sequence voltages of that bus. In detail, if vector $\mathbf{u}_m$ carries the voltage phasors at the three phases of bus $m \in \mathcal{M}$, the VUF factor can be computed as

$$\omega_m = \frac{|V_m^-|}{|V_m^+|} = \frac{|\boldsymbol{\rho}^H \mathbf{u}_m|}{|\boldsymbol{\rho}^\top \mathbf{u}_m|} \tag{11}$$

where $\boldsymbol{\rho} := [1 \ e^{j\frac{2\pi}{3}} \ e^{j\frac{4\pi}{3}}]^\top$. According to IEC, the VUF should be maintained below 2%. Reducing phase imbalance can be critical for the operation of large three-phase motors. Although DERs may be approximately uniformly distributed across phases, imbalances in power injections during real-time operation may result in phase imbalance. Additionally, reactive power injections attempting to regulate voltage magnitudes may inadvertently exacerbate voltage imbalance.

To address these concerns, we incorporate voltage balance constraints into the ORD problem. For specific three-phase buses, consider the constraint

$$\Pr_{\boldsymbol{\theta}}\left(\omega_m(\mathbf{z};\boldsymbol{\theta}) \leq 0.02\right) \geq 1-\beta_2, \ \forall m \in \mathcal{M}. \tag{12}$$

While voltage magnitude constraints are enforced per node, voltage imbalance constraints are enforced per bus. If the voltage imbalance constraint is rearranged as $|\boldsymbol{\rho}^H \mathbf{u}_m|^2 \leq 0.02^2 \cdot |\boldsymbol{\rho}^\top \mathbf{u}_m|^2$, it can be alternatively expressed as

$$\Pr_{\boldsymbol{\theta}}(\mathbf{u}^H \boldsymbol{\Phi}_m \mathbf{u} \leq 0) \geq 1-\beta_2, \ \forall m \in \mathcal{M} \tag{13}$$

where $\boldsymbol{\Phi}_m := \mathbf{S}_m(\boldsymbol{\rho}\boldsymbol{\rho}^H - 0.02^2 \cdot \boldsymbol{\rho}^*\boldsymbol{\rho}^T)\mathbf{S}_m^\top$, and $\mathbf{S}_m$ is a selection matrix to obtain $\mathbf{u}_m$ from $\mathbf{u}$ as $\mathbf{u}_m = \mathbf{S}_m^\top \mathbf{u}$. We can again use the logistic function to simplify (13) as

$$\mathbb{E}_{\boldsymbol{\theta}}\left[\tilde{\mathbb{1}}_\gamma(\mathbf{u}_m^H \boldsymbol{\Phi} \mathbf{u}_m)\right] \leq \beta_2 \tag{14}$$

Constraints (10) and (14) can be enforced on suitable nodes and buses, and are substituted in (6) to give rise to a stochastic optimization problem. Solving this problem, however, is challenging as the probability density function of $\boldsymbol{\theta}$ is unknown. This challenge is addressed next using the standard technique of stochastic sample approximation.

IV. Solution Methodology

The expectation appearing in the objective and constraints in (10) and (14), can be approximated by sample averages:

$$\mathbb{E}_{\boldsymbol{\theta}}\left[\ell(\mathbf{z};\boldsymbol{\theta})\right] \simeq \frac{1}{S}\sum_{s=1}^{S} \ell(\mathbf{z};\boldsymbol{\theta}_s)$$

where $\{\boldsymbol{\theta}_s\}_{s=1}^S$ is a set of representative grid scenarios anticipated for the next two hours. Therefore, VVR rule parameters can be optimized by solving the problem

$$\begin{aligned} \min_{\mathbf{z}\in\mathcal{Z}_\epsilon} \quad & \frac{1}{S}\sum_{s=1}^{S} \ell(\mathbf{z};\boldsymbol{\theta}_s) \\ \text{s.to} \quad & \frac{1}{S}\sum_{s=1}^{S} g_c(\mathbf{z};\boldsymbol{\theta}_s) \leq \beta, \ \forall c \in \mathcal{C}. \end{aligned} \tag{15}$$

The function g_c represents the function inside the expectation operator in (10) and (14). Because objective and constraints are differentiable, problem (15) can be solved using the projected primal-dual decomposition method.

The Lagrangian function of problem (15) is

$$L(\mathbf{z};\boldsymbol{\lambda}) = \frac{1}{S}\sum_{s=1}^{S} \ell(\mathbf{z};\boldsymbol{\theta}_s) + \sum_{c\in\mathcal{C}} \lambda_c \left(\frac{1}{S}\sum_{s=1}^{S} g_c(\mathbf{z};\boldsymbol{\theta}_s) - \beta\right)$$

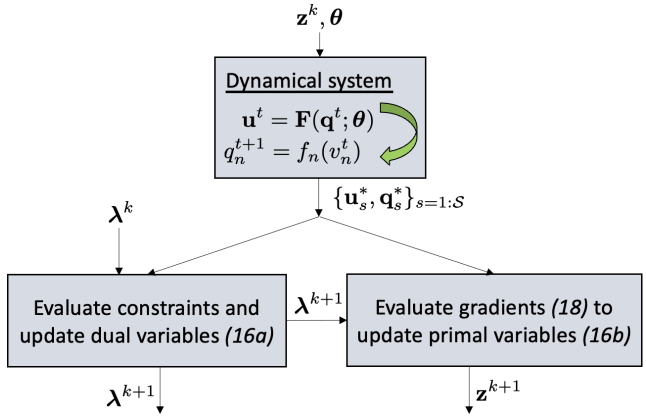

Fig. 3. Overview of the proposed algorithm for optimizing VVR rule parameters in multiphase feeders. Given the current iterate of VVR parameters $\mathbf{z}^k$ and for each grid loading scenario $\boldsymbol{\theta}$, we find the grid equilibrium state by iterating between the PF problem and the VVR rules. Constraints are evaluated across all scenarios and passed into the logistic function to update dual variables. Primal variables are updated by linearly combining Lagrange multipliers and constraint gradients.

where λ_c is the Lagrange multipliers corresponding constraint c. Lagrange multipliers are collected in vector $\boldsymbol{\lambda}$. The primal-dual decomposition method seeks to minimize L over primal variables $\mathbf{z} \in \mathcal{Z}_\epsilon$, and maximize L over dual variables $\boldsymbol{\lambda} \geq \mathbf{0}$. This is accomplished using successive primal gradient descent and dual gradient ascent iterations:

$$\lambda_c^{k+1} = \left[\lambda_c^k + \mu_\lambda \left(\frac{1}{S}\sum_{s=1}^{S} g_c(\mathbf{z}^k;\boldsymbol{\theta}_s) - \beta\right)\right]_+, \ \forall c \in \mathcal{C} \tag{16a}$$

$$\mathbf{z}^{k+1} := \left[\mathbf{z}^k - \mu_z \nabla_{\mathbf{z}} L(\mathbf{z}^k;\boldsymbol{\lambda}^{k+1})\right]_{\mathcal{Z}_\epsilon} \tag{16b}$$

where k denotes the iteration number and (μ_z, μ_λ) are positive step sizes. Primal variables $\mathbf{z}$ are projected onto set $\mathcal{Z}_\epsilon$, while operator $[\cdot]_+$ ensures the non-negativity of dual variables. The updated primal variable $\mathbf{z}^{k+1}$ is fed back to the dynamical system (3) to obtain new equilibrium states.

Gradient $\nabla_{\mathbf{z}} g_c$ can be calculated using the chain rule as:

$$(\nabla_{\mathbf{z}} g_c)^\top = (\nabla_{\mathbf{u}} g_c)^\top \cdot \nabla_{\mathbf{q}}\mathbf{u} \cdot \nabla_{\mathbf{z}}\mathbf{q}. \tag{17}$$

Knowing that the PF equations map $\mathbf{u}$ to power injections $\mathbf{s}$, we can use the inverse function theorem to compute

$$(\nabla_{\mathbf{z}} g_c)^\top = (\nabla_{\mathbf{u}} g_c)^\top \cdot (\nabla_{\mathbf{u}}\mathbf{s})^{-1} \cdot \mathbf{T} \cdot \nabla_{\mathbf{z}}\mathbf{q} \tag{18}$$

where matrix $\mathbf{T}$ selects the columns from the inverse Jacobian $\nabla_{\mathbf{s}}\mathbf{u}$ corresponding to $\nabla_{\mathbf{q}}\mathbf{u}$. We next elaborate on computing the components appearing in (18).

1) Evaluating $\nabla_{\mathbf{z}}\mathbf{q}$: Determining the Jacobian $\nabla_{\mathbf{z}}\mathbf{q}$ involves differentiating the VVR control rules $\mathbf{f}(\mathbf{z};\mathbf{v})$ with respect to $\mathbf{z}$. Note that $\mathbf{f}$ is a function of both $\mathbf{z}$ and voltage $\mathbf{v}$, which, in turn, depends on $\mathbf{q}$ through the PF equations. Therefore, to differentiate over the implicit equation $\mathbf{q} = \mathbf{f}(\mathbf{z};\mathbf{v})$, we must use total differentiation [15]:

$$\nabla_{\mathbf{z}}\mathbf{q} = \frac{\partial \mathbf{f}}{\partial \mathbf{v}} \cdot (\nabla_{\mathbf{z}}\mathbf{v}) + \frac{\partial \mathbf{f}}{\partial \mathbf{z}} \cdot \nabla_{\mathbf{z}}\mathbf{z}$$

$$= \frac{\partial \mathbf{f}}{\partial \mathbf{v}} \cdot (\nabla_{\mathbf{u}} \mathbf{v} \cdot \nabla_{\mathbf{q}} \mathbf{u} \cdot \nabla_{\mathbf{z}} \mathbf{q}) + \frac{\partial \mathbf{f}}{\partial \mathbf{z}} \cdot \mathbf{I}.$$

After some trivial manipulations, we get that

$$\nabla_{\mathbf{z}} \mathbf{q} = \left(\mathbf{I} - \frac{\partial \mathbf{f}}{\partial \mathbf{v}} \cdot \nabla_{\mathbf{u}} \mathbf{v} \cdot \nabla_{\mathbf{q}} \mathbf{u} \right)^{-1} \cdot \frac{\partial \mathbf{f}}{\partial \mathbf{z}}$$

2) Evaluating $\nabla_{\mathbf{u}} \ell$ and $\nabla_{\mathbf{u}} g_c$: Ohmic losses can be expressed as the sum of active power injections across all nodes. As such, they can be expressed as a quadratic function of $\mathbf{u}$, and thus, the gradient $\nabla_{\mathbf{u}} \ell$ can be readily computed. The gradient $\nabla_{\mathbf{u}} g_c$ for constraints related to voltage magnitude violations as in (10) can be computed as:

$$\nabla_{\mathbf{u}} g_c = \frac{1}{\gamma} \cdot g_c \cdot (1 - g_c) \cdot 2(v_c - 1) \cdot \nabla_{\mathbf{u}} v_c.$$

The formula can be obtained by differentiating the logistic function and applying the chain rule. The gradient $\nabla_{\mathbf{u}} g_c$ for constraints related to voltage imbalance as in (14) is:

$$\nabla_{\mathbf{u}} g_c = \frac{1}{\gamma} \cdot g_c \cdot (1 - g_c) \cdot 2\mathbf{u}_c^T \cdot \mathbf{\Phi} \cdot \nabla_{\mathbf{u}} \mathbf{u}_c.$$

Figure 3 depicts the workflow of the algorithm.

V. Numerical Tests

The proposed method was numerically evaluated using the IEEE 37-bus multi-phase feeder, wherein all buses are three-phase nodes. Real-world active load demands and solar generation were obtained from the Smart* project at one-minute intervals for April 2, 2011 [20]. The dataset contains active load demands from 443 houses and solar generation from 50 rooftop solar panels. The testing dataset was created by randomly selecting homes and assigning them to the non-zero injection nodes of the benchmark feeder. Each load time series was normalized so its peak value equals 3 times the nominal active load of the corresponding node. This accommodates the anticipated load growth due to electrified vehicles and/or heating. Because the original dataset does not include kVAR demands, reactive power injections were simulated based on the active power loads and the power factors reported by the benchmark. Solar generation was scaled so its maximum daily value is 3 times the peak load demand based on the original benchmark loads. We added single-phase DERs on non-zero load nodes as shown in Fig. 4. To evaluate the performance of the proposed method, we conducted tests during the 11:30—13:30 period, during which solar generation exhibited high fluctuations due to clouds. This period includes 120 scenarios. To generate additional scenarios, we introduced small perturbations by adding zero-mean Gaussian noise with a variance of 0.001 to 30 randomly selected scenarios.

All tests were conducted on a laptop computer with an Apple M3 Pro processor and 32GB of RAM. The control rules were designed and evaluated using MATLAB R2022a, with YALMIP and Gurobi 11.0 employed for the projection step. The rule parameters were initialized as $(\bar{v}_n, \delta_n, \sigma_n, \alpha_n) = (1.00, 0.1, 0.06, \frac{\bar{q}_n}{\sigma_n - \delta_n})$ for all n, and the stability margin ϵ was set to 0.1. Iterations were terminated when the relative error between consecutive parameter updates $\mathbf{z}$ became less than 10^{-6}. Upon experimentation, step sizes were chosen as $\mu_z = 0.1 \cdot 0.99^k$ and $\mu_\lambda = 0.01 \cdot 0.99^k$, respectively.

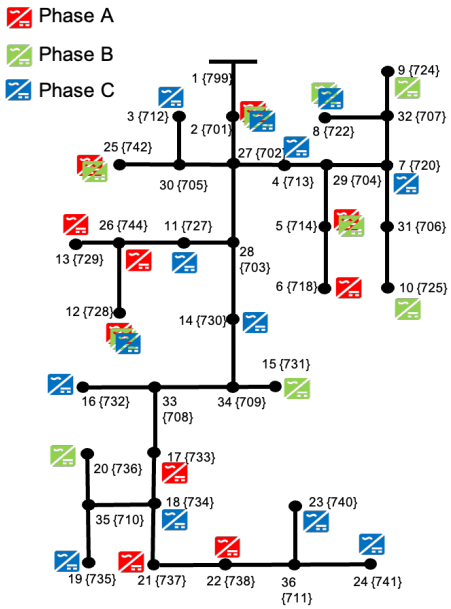

Fig. 4. Single-phase DERs with VVR control capabilities added to the IEEE 37-bus multi-phase feeder.

To evaluate our ORD methodology, we tested four design options: *a)* No VVR control; *b)* VVR rules designed for $(\beta_1, \beta_2) = (0.2, 1.0)$; *c)* VVR rules designed for $(\beta_1, \beta_2) = (0.1, 1.0)$; and *d)* VVR rules designed for $(\beta_1, \beta_2) = (0.1, 0.1)$. Figure 5 presents the histograms of voltage magnitudes for all nodes and VUF metrics for all three-phase buses, across the four design options *a)-d)*. Under option *a)*, voltage magnitudes exceed the limit of $\pm 3\%$ for several nodes and scenarios, and the VUF exceeds 2% for several buses, too. Compared to option *a)*, option *b)* shows a decrease in the probability of voltage magnitudes exceeding the $\pm 3\%$ limit, although the VUF increases. This trend becomes more pronounced under option *c)*, where voltage magnitudes are more tightly distributed within the range of $[0.97, 1.03]$, but the probability of the VUF exceeding 2% is higher than in *b)*. In contrast, option *d)* improves both voltage magnitude and VUF, with the maximum violation probabilities reduced to 10%. Table I summarizes ohmic losses and the worst-case probabilities of voltage violation and imbalance violation across all scenarios for different values of (β_1, β_2). As the values of (β_1, β_2) decrease, the worst-case probabilities decrease accordingly, while the ohmic losses increase, as expected.

TABLE I
Worst-Case Probabilities and Ohmic Losses

(β_1,β_2)	Voltage Probability [%]	Imbalance Probability [%]	Ohmic Losses [kW]
(0.2,1.0)	20.11	34.77	46.91
(0.2,0,2)	19.99	19.81	46.95
(0.1,1.0)	10.20	40.37	47.99
(0.1,0.2)	11.47	20.42	49.41
(0.1,0.1)	11.60	10.87	53.88

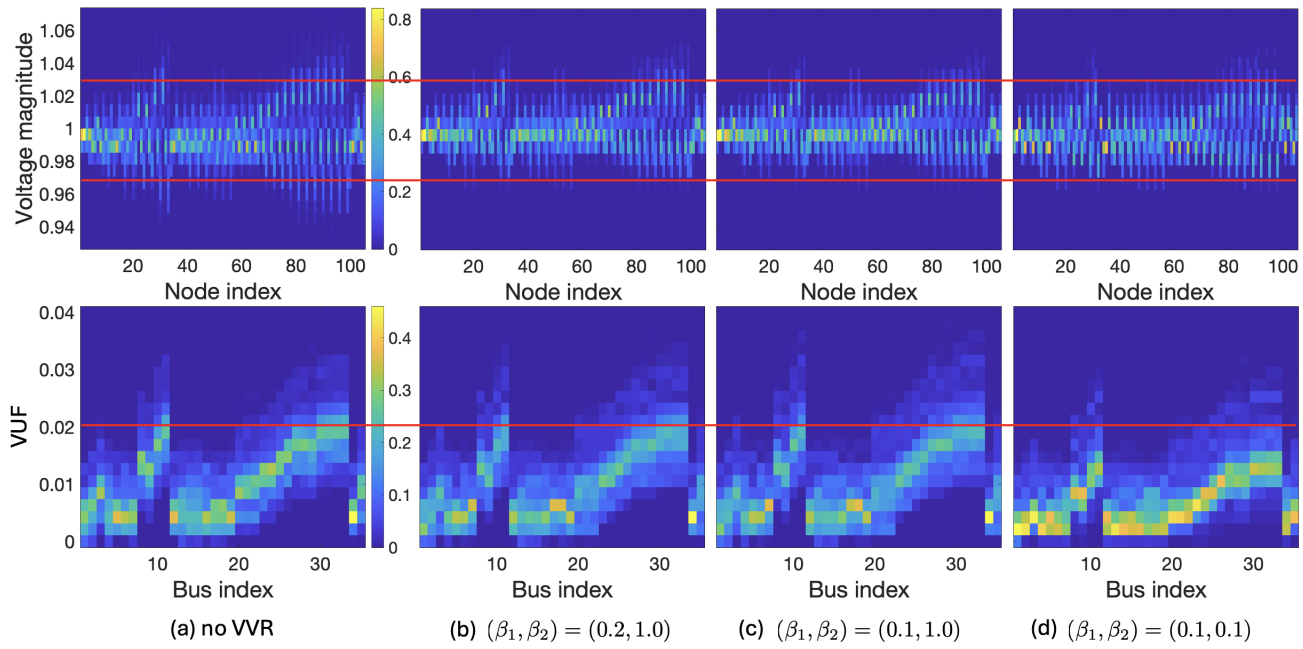

Fig. 5. Histograms of voltage magnitude and VUF for various (β_1, β_2) settings. From *a)* to *b)*, magnitudes become more tightly regulated. In *c)*, magnitudes are further confined at the expense of wider voltage imbalance violations. Panel *d)* attains tighter regulation in voltage magnitude and imbalance alike.

VI. Conclusions

This work has devised a chance-constrained ORD formulation to minimize ohmic losses in multiphase distribution feeders. The formulation incorporates chance constraints on voltage magnitude and imbalance to address issues arising from the uncertainty of load and solar power injections. A primal-dual gradient algorithm has been proposed to find near-optimal VVR rule parameters. Numerical tests using real-world load and solar data on the IEEE-37 feeder validate the effectiveness of the proposed method in ORD while satisfying chance constraints. To further improve upon computational complexity, one could explore stochastic primal-dual algorithms and attempt to avoid the nested loop incurring with the dynamical loop and the AC-PF solver.

References

[1] M. Farivar, R. Neal, C. Clarke, and S. Low, "Optimal inverter VAR control in distribution systems with high PV penetration," in *Proc. IEEE Power & Energy Society General Meeting*, San Diego, CA, Jul. 2012.

[2] *IEEE Standard for Interconnection and Interoperability of DERs with Associated Electric Power Systems Interfaces*, IEEE Std., 2018.

[3] G. Cavraro, S. Bolognani, R. Carli, and S. Zampieri, "The value of communication in the voltage regulation problem," in *Proc. IEEE Conf. on Decision and Control*, 2016, pp. 5781–5786.

[4] R. A. Jabr, "Segregated linear decision rules for inverter Watt-VAr control," *IEEE Trans. Power Syst.*, vol. 36, no. 3, pp. 2702–2708, 2021.

[5] S. Gupta, V. Kekatos, and S. Chatzivasileiadis, "Optimal design of Volt/VAR control rules of inverters using deep learning," *IEEE Trans. Smart Grid*, vol. 15, no. 5, pp. 4731–4743, Sep. 2024.

[6] X. Zhou, J. Tian, L. Chen, and E. Dall'Anese, "Local voltage control in distribution networks: A game-theoretic perspective," in *2016 North American Power Symposium (NAPS)*, Nov 2016, pp. 1–6.

[7] X. Zhou, M. Farivar, Z. Liu, L. Chen, and S. H. Low, "Reverse and forward engineering of local voltage control in distribution networks," *IEEE Trans. Autom. Contr.*, vol. 66, no. 3, pp. 1116–1128, 2021.

[8] R. Xu, C. Zhang, Y. Xu, Z. Dong, and R. Zhang, "Multi-objective hierarchically-coordinated volt/var control for active distribution networks with droop-controlled pv inverters," *IEEE Trans. Smart Grid*, vol. 13, no. 2, pp. 998–1011, Mar 2022.

[9] A. Inaolaji, A. Savasci, and S. Paudyal, "Optimal droop settings of smart inverters," in *IEEE Photovoltaic Specialists Conference*, 2021, pp. 2584–2589.

[10] A. Savasci, A. Inaolaji, and S. Paudyal, "Distribution grid optimal power flow with adaptive Volt-VAr droop of smart inverters," in *IEEE Industry Applications Society Annual Meeting*, Vancouver, BC, 2021, pp. 1–8.

[11] J. Wei, S. Gupta, D. C. Aliprantis, and V. Kekatos, "A chance-constrained optimal design of Volt/VAR control rules for distributed energy resources," in *Proc. North American Power Symposium*, Ashville, NC, Oct. 2023.

[12] K. Baker, A. Bernstein, E. Dall'Anese, and C. Zhao, "Network-cognizant voltage droop control for distribution grids," *IEEE Trans. Power Syst.*, vol. 33, no. 2, pp. 2098–2108, 2018.

[13] J. Sepulveda, A. Angulo, F. Mancilla-David, and A. Street, "Robust co-optimization of droop and affine policy parameters in active distribution systems with high penetration of photovoltaic generation," *IEEE Trans. Smart Grid*, vol. 13, no. 6, pp. 4355–4366, 2022.

[14] A. Inaolaji, A. Savasci, and S. Paudyal, "Distribution grid optimal power flow in unbalanced multiphase networks with Volt-VAr and Volt-Watt droop settings of smart inverters," *IEEE Trans. Ind. Applicat.*, vol. 58, no. 5, pp. 5832–5843, 2022.

[15] I. Murzakhanov, S. Gupta, S. Chatzivasileiadis, and V. Kekatos, "Optimal design of Volt/VAR control rules for inverter-interfaced distributed energy resources," *IEEE Trans. Smart Grid*, vol. 15, no. 1, pp. 313–323, Jan. 2023.

[16] M. Yao, I. A. Hiskens, and J. L. Mathieu, "Mitigating voltage unbalance using distributed solar photovoltaic inverters," *IEEE Trans. Power Syst.*, vol. 36, no. 3, pp. 2642–2651, 2021.

[17] K. Girigoudar, A. M. Hou, and L. A. Roald, "Chance-constrained AC optimal power flow for unbalanced distribution grids," in *Bulk Power Systems Dynamics and Control Symposium*, Banff, CANADA, Jul. 2022.

[18] M. Bazrafshan and N. Gatsis, "Comprehensive modeling of three-phase distribution systems via the bus admittance matrix," *IEEE Trans. Power Syst.*, vol. 33, no. 2, pp. 2015–2029, 2018.

[19] P. Jahangiri and D. C. Aliprantis, "Distributed Volt/VAr control by PV inverters," *IEEE Trans. Power Syst.*, vol. 28, no. 3, pp. 3429–3439, Aug. 2013.

[20] D. Chen, S. Iyengar, D. Irwin, and P. Shenoy, "Sunspot: Exposing the location of anonymous solar-powered homes," in *ACM Intl. Conf. on Systems for Energy-Efficient Built Environ.*, Palo Alto, CA, Nov. 2016.